PERFORMANCE OF THE CMIP6 GLOBAL CLIMATE MODELS OVER THE IBERIAN PENINSULA AND RELATIONSHIPS WITH THE SIMULATED CLIMATE SYSTEM COMPLEXITY

Swen BRANDS[1], Juan A. FERNÁNDEZ-GRANJA[2], Jesús FERNÁNDEZ[2] , Joaquín BEDIA[2], Ana CASANUEVA[2] , Juan J. TABOADA[1]
1 MeteoGalicia, Consellería de Medio Ambiente, Territorio y Vivienda - Xunta de Galicia, 15707 Santiago de Compostela, Spain
2 Meteorology Group, Department of Applied Mathematics and Computer Science, University of Cantabria, 39005, Santander, Spain
swen.brands@gmail.com

RESUMEN
En el presente estudio se muestra una evaluación del rendimiento de las diferentes configuraciones de los modelos climáticos globales que han aportado experimentos históricos a CMIP6 (Coupled Model Intercomparison Project 6) para la Península Ibérica (IB), utilizando un dominio similar al aplicado en iniciativas de downscalling anteriores. La evaluación se basa en los patrones típicos de circulación atmosférica regional definidos por Jenkinson y Collison (1977), que se sabe que están vinculados con un gran número de variables de la física y la química atmosféricas. Los resultados se comparan con los obtenidos de la generación anterior de los modelos (CMIP5) y con los obtenidos de un análisis hemisférico (Brands 2022a), para comprobar 1) si los modelos han mejorado con el tiempo y 2) si los resultados específicos concuerdan con los obtenidos en un dominio más grande, lo que los hace menos propensos a la propagación de errores durante períodos de tiempo no observados. Los resultados indican que los cambios de versión del modelo de CMIP5 a 6 conducen a ligeras mejoras, principalmente asociadas a un aumento en la resolución del modelo horizontal, pero que la selección de la familia de modelos adecuada es más importante para obtener un buen rendimiento del modelo. Los resultados también se clasifican con una puntuación simple que describe la complejidad de los modelos climáticos globales en términos de componentes prescritos e interactivos del sistema climático (Brands 2022a). Dado que, en principio, son preferibles representaciones más completas del sistema climático a otras más simples, y también producen características únicas en las proyecciones futuras, se propone esta puntuación como punto de partida para considerar la complejidad del sistema climático como criterio adicional de selección del modelo. El estudio hace uso de un amplio archivo de metadatos, describiendo los modelos globales acoplados con detalle (https://github.com/SwenBrands/gcm-metadata-for-cmip)

Palabras clave: CMIP6, CMIP5, modelos climáticos globales, bondad, grado de complejidad, Península Ibérica, reanálisis

ABSTRACT
A performance assessment of the global climate model configurations contributing historical experiments to CMIP6 is provided for the Iberian Peninsula (IB), using a spatial domain similar to that applied in previous downscaling initiatives. The evaluation is based on typical recurrent regional atmospheric circulation patterns as defined by Jenkinson & Collison (1977), which are well known to be linked with a large number of variables from atmospheric physics and chemistry. Results are compared to those obtained from the previous model generation (CMIP5), and to those retrieved from a hemispheric-wide analysis (Brands 2022) in order to see 1) if the models have improved over time, and 2) whether the region-specific findings agree with those obtained on a larger domain, thereby making them less prone to error propagation during unobserved time periods. It is found that the model version changes from CMIP5 and 6 lead to slight improvements, mainly associated with an increase in horizontal model resolution, but that the selection of the right model family is more important to obtain good model performance. The results are also put into relation with a simple score describing the global climate models' *complexity* in terms of prescribed and interactive climate system components (Brands 2022). Since more complete representations of the climate system are in principle preferable to simpler ones, and also produce unique scenario features, this score is proposed as starting point to consider *climate system complexity* as additional model selection criterion. Since model performance is found to be unrelated to model complexity, this an argument for the use of the more realistic model configurations, described with detail in an exhaustive metadata archive developed in collaboration with the model developers themselves (https://github.com/SwenBrands/gcm-metadata-for-cmip).

Key words: CMIP6, CMIP5, global climate models, model performance, model complexity, Iberian Peninsula, reanalysis data

1. INTRODUCTION

Global climate models (GCMs) are complex code packages including up to a dozen of individual component models, each of which simulating usually one specific realm of the climate system, with varying degrees of coupling between these sub-models. Developed since the late 1960ies, GCMs are nowadays being used following two general strategies. The first makes use of only a few sub-models usually covering the physical processes of the four basic realms "atmosphere", "land-surface", "ocean" and "sea-ice" and concentrates the available computational resources on a resolution as fine as possible. The second "Earth System Model" approach works the other way around. Therein, the number of applied sub-models are maximized in order to obtain a simulated climate system as comprehensive as possible, going beyond the pure physical processes, at the expense of model resolution (Kawamiya et al. 2020).
The thereby growing diversity of coupled model configurations makes it necessary to provide detailed model metadata to avoid "black-box" use and to pipe specific model configurations to the corresponding user needs. Air quality applications, for instance, ideally require atmospheric chemistry and aerosols to be interactively resolved and coupled to each other in the model world. Corresponding efforts to shed light on the

many available GCM setups are under-way (e.g. https://es-doc.org/), but only cover the model configurations used in CMIP6 (Eyring et al. 2016). Thus, recovering metadata for earlier CMIP generations can be in a way compared with the rescue of early station data.

The present study is a recompilation and update of the GCM performance atlas provided for the northern hemisphere (NH) extra-tropics in Brands (2022a), tailored to the needs of regional climate science for the Iberian Peninsula (IB). *Sixty* global climate model configurations used in CMIP5 and 6 (Taylor et al. 2011, Eyring et al. 2016) are assessed in terms of their capacity to reproduce the climatological frequencies (1979-2005) of the 27 Lamb weather types (LWTs) describing recurrent sea-level pressure patterns in that region (Jenkinson & Collison 1977). These weather types are well known to be associated with a number of key variables in atmospheric physics and chemistry, whose state is driven by the synoptic wind or lack thereof (e. g. temperature, precipitation, fog, ozone and particulate matter concentrations etc.). First, a GCM ranking is provided for a study area similar to that used in previous national downscaling projects (Fernández et al. 2019). Then, the IB results are compared with the NH results obtained from Brands (2022a) in order to check for possible scale-dependencies and tuning issues. Furthermore, model performance is put into relation with *model complexity* in terms of represented climate system components, which may be used as additional model selection criterion. Following the rationale of the Fernández-Granja et al. (2022) contribution to this congress series, it is finally shown that the performance of some of the most commonly used GCMs is clearly enhanced when being evaluated against specific reanalysis datasets, pointing to the need of searching for independent reference datasets. The study makes use of an extensive GCM metadata archive built with the help of the model development teams themselves.

2. DATA AND METHODS

For the present study, the six-hourly LWT catalogues built in Brands (2022a) and stored at Brands (2022b) were extented by four additional GCMs and one reanalysis dataset (ERA5, Hersbach et al. 2020) and then recompiled for a spatial domain covering southwestern Europe, covering an area between 40W-35E and 30N-60N, hereafter referred to as the "IB domain" (see Figure 1). An overview of the applied GCM runs is given in Appendix and a complete description, including reference articles and the specifications of *all* sub-models, is provided at Brands (2022c, see *get_historical_metadata.py* function therein). Here, *model performance* is defined as the Mean Absolute Error (MAE) of the relative frequencies for the 27 LWTs simulated by a given GCM with respect to a given reanalysis.

$$MAE = \frac{1}{n}\sum_{i=1}^{n}[m_i - o_i] \quad (1)$$

, where m_i and o_i are the modelled and quasi-observed relative frequencies of the i^{th} type out of a total of n = 27 Lamb weather types. The MAE is expressed in percent. Since the EC-Earth model family makes use of the same atmospheric general circulation model as the ECMWF reanlayses (see Appendix), the primary reference

dataset used here is the JRA-55 reanalysis (Kobayashi et al. 2015), assumed to be more independent.

Equation 1 is applied for each grid-box of the 2.5 degrees latitude-longitude grid covering the IB domain (Figure 1), thereby obtaining 403 MAE values for each GCM. In the forthcoming, these are mapped or summarized in a boxplot, in which case the median and interquartile range (IQR) of the error sample per GCM are shown, as well as the whiskers placed at the 75th percentile plus 1.5 times the IQR and at the 25th percentile minus 1.5 times the IQR, respectively (Brands et al. 2021).

As proposed in Brands (2022a), the complexity of the considered coupled model configurations is summarized in a single code containing 10 integers. Each integer represents a specific component of the climate system in the following order: 1. Atmosphere, 2. Land-surface, 3. Ocean, 4. Sea-ice, 5. Vegetation, 6. Terrestrial carbon-cycle processes, 7. Aerosols, 8. Atmospheric chemistry, 9. Ocean carbon-cycle processes and 10. Ice-sheet dynamics. The integer is set to 0 if the component is not taken into account at all, to 2 if it is simulated by a an interactive sub-model that is coupled to at least one other sub-model representing another climate system component, and to 1 for anything in between, including prescription from external files or "semi-interactive" sub-models. Note that the initial code estimates derived from the model output files and reference articles were sent to the model development teams themselves for confirmation. This led to a community effort whose current state is reflected by the git repository "gcm-metadata-for-cmip" available at https://github.com/SwenBrands/gcm-metadata-for-cmip

As an example, the integer code for EC-Earth3, the basic EC-Earth configuration used in CMIP6, is 2222001000, indicating interactive atmosphere, land-surface, ocean and sea-ice sub-models and prescribed aersols. EC-Earth3-CC is the more comprehensive carbon-cycle version of this model family, which additionally comprises interactive sub-models for vegetation properties as well as carbon-cycle processes over land and ocean. This is reflected by the integer code 2222221020.

The sum of the integer code is used as a summary measure of model complexity as defined above, with larger sums indicating higher complexity (see Appendix). For the examples mentioned below, EC-Earth3 and EC-Earth3-CC receive complexity scores of 9 and 15, respectively. Remarkably, none of the sixty considered GCMs contains an interactive representation of ice-sheet dynamics albeit their key importance for the climate system.

An in-depth analysis of the model metadata gathered at https://github.com/SwenBrands/gcm-metadata-for-cmip revealed that the number of independent component models for e.g. the atmosphere is much lower than the number of nominally different GCMs (see Appendix). Likewise, the GCMs particpating for the first time in CMIP6 (KIOST-ESM, SAM0-UNICON, TaiESM1, NESM3, KACE-1-0-G) are essentially modified versions of the Community Earth System Model (CESM), the Max Planck Institute Earth System Model (MPI-ESM), or the Geophysical Fluid Dynamics Atmospheric Model (GFDL-AM), with the exception of IITM-ESM (see also Table 1 in Brands 2022a).

3. RESULTS

Figure 1 shows the grid-box-scale MAE values mapped over the IB domain and the associated ranks for five candidate GCMs from two distinct model families, being generally representative for the behaviour of the entire multi-model ensemble considered here. Model version changes from CMIP5 to 6 (from EC-Earth2.3 to EC-Earth3 and from IPSL-CM5A-LR to IPSL-CM6A-LR in Figure 1) leads to performance gains for both families whilst an increase in model complexity (from EC-Earth3 to EC-Earth3-CC), associated with a considerable increase in potential error sources, does not largely deteriorate the results.

Figure 2 shows the summary results for each of the 60 considered GCMs by means of a boxplot. The four items displayed on the right of the figure (in light green) refer to the joint samples of the *more* and the *less* complex GCM configurations from *CMIP5* and *6*, respectively, using a complexity-score threshold of 14 (Brands 2022a). It can be seen that the aforementioned version changes are generally less important for model performance than the choice of the right model family. This is underlined by the finding that the *CMIP6* versions of the five "worse" performing families (FGOALS, BCC-CSM, GISS-E2, IPSL-CM, MIROC) yield larger median errors than the *CMIP5* versions of the six "well" performing familes (ACCESS, HadGEM, EC-Earth, CNRM-CM, GFDL-CM/ESM and MRI-ESM). This can be partly explained with the horizontal resolution of the atmospheric sub-models, which, for the 6 well performing models, was already relatively high in CMIP5 (see also Figure 5a).

To assess the effects of internal model variability arising from variations in the initial conditions, 72 addiontal runs from a sub-set of 13 distinct GCMs were evaluated in addition (Figure 3). As expected, these effects are larger on average over the IB domain than over the larger northern-hemisphere domain (NH, see Brands 2022a), but nevertheless much smaller then the inter-model variability observed in Figure 2.

Figure 4 plots the median model performance for the IB domain against the corresponding values for the NH domain, taken from Brands (2022a). As revealed by a Pearson correlation coefficient of 0.87, the results for the two domains generally agree if the errors are standardized and thus corrected for differences in magnitude and dispersion, which may arise from the different orographic characteristics and land-sea distributions of the two domains.

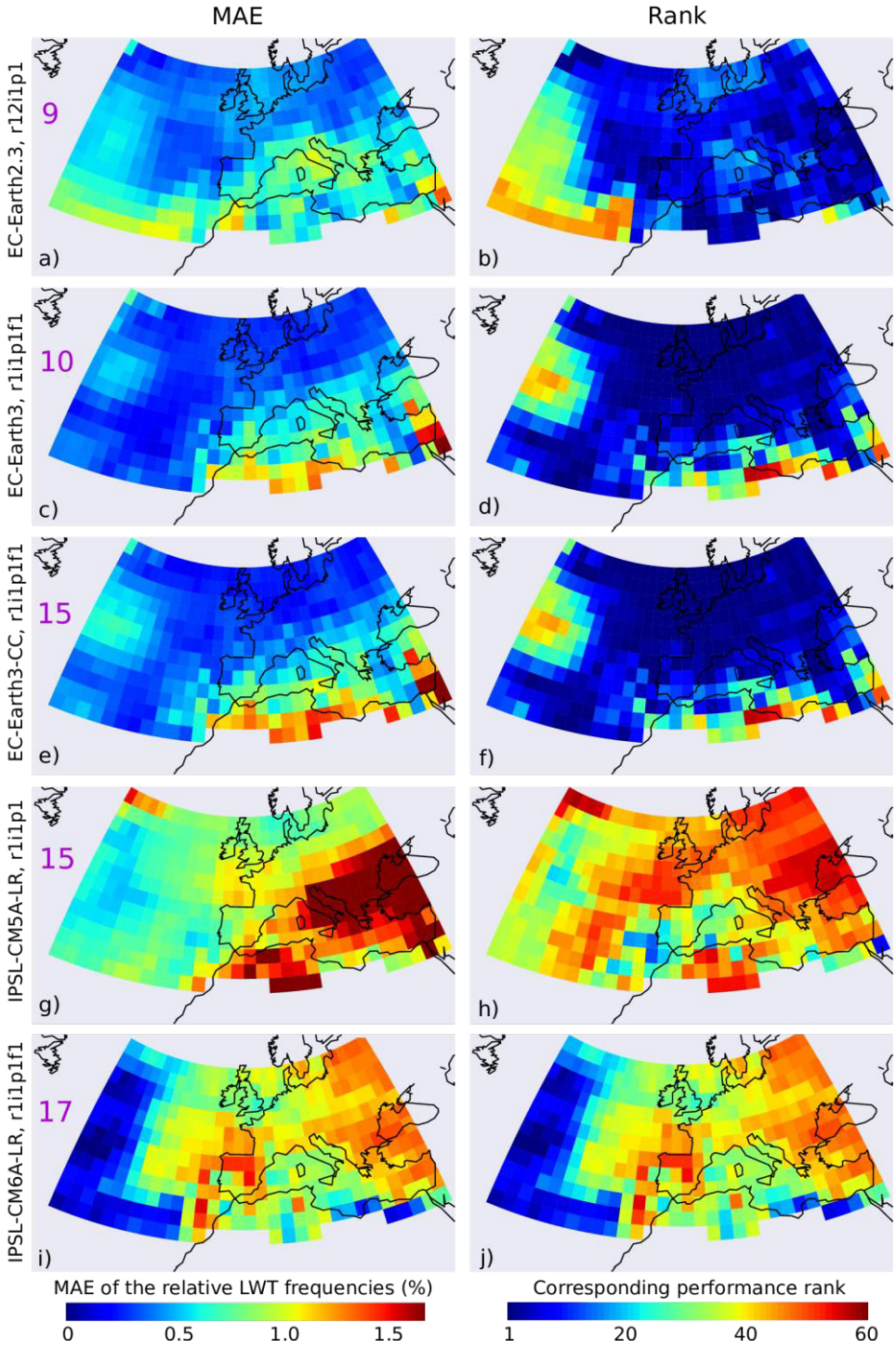
MAE
Rank
EC-Earth2.3, r12i1p1
9
a)
b)
EC-Earth3, r1i1p1f1
10
c)
d)
EC-Earth3-CC, r1i1p1f1
15
e)
f)
IPSL-CM5A-LR, r1i1p1
15
g)
h)
IPSL-CM6A-LR, r1i1p1f1
17
i)
j)
MAE of the relative LWT frequencies (%)
0
0.5
1.0
1.5
Corresponding performance rank
1
20
40
60

Fig. 1: Mean Absolute Error of the 27 climatological Lamb weather type frequencies (1979-2005) w.r.t. JRA-55 for 5 candidate GCMs (left column), as well as the corresponding performance ranks (1 = best, 60 = worst, right domain) over the Iberian Peninsula domain. Purple numbers indicate model complexity scores.

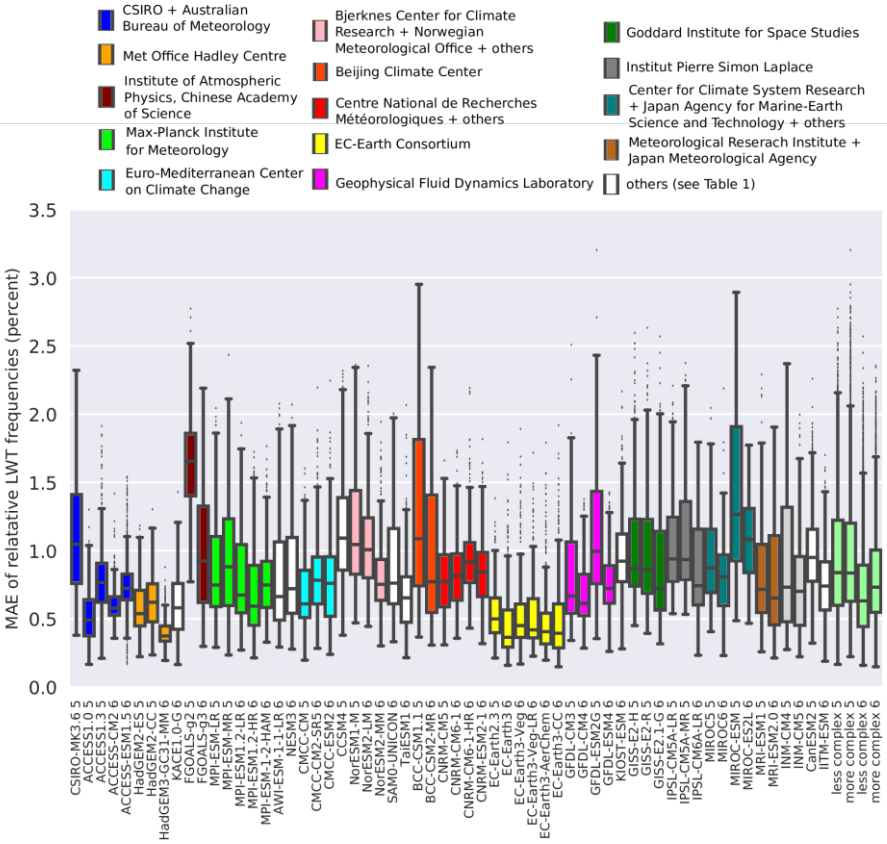

Fig. 2: Distribution of the grid-box scale Mean absolute errors (%) over the Iberian Peninsula domain for each of the 60 considered GCM configuration. Each boxplot-item is a summary of the the mapped errors, as illustrated in Figure 1. The CMIP generation (either 5 or 6) is indicated after the model acronym. Results are with respect to JRA-55.

Performance is generally better over ocean than over land masses and particularly poor over large orographic barriers where, at the same time, reanalysis uncertainty is largest (Fernández-Granja et al. 2022, contribution to this congress series). The close agreement documented by Figure 4 points to the fact that the GCMs have likely not been tuned to fit the regional atmospheric circulation in the NH.

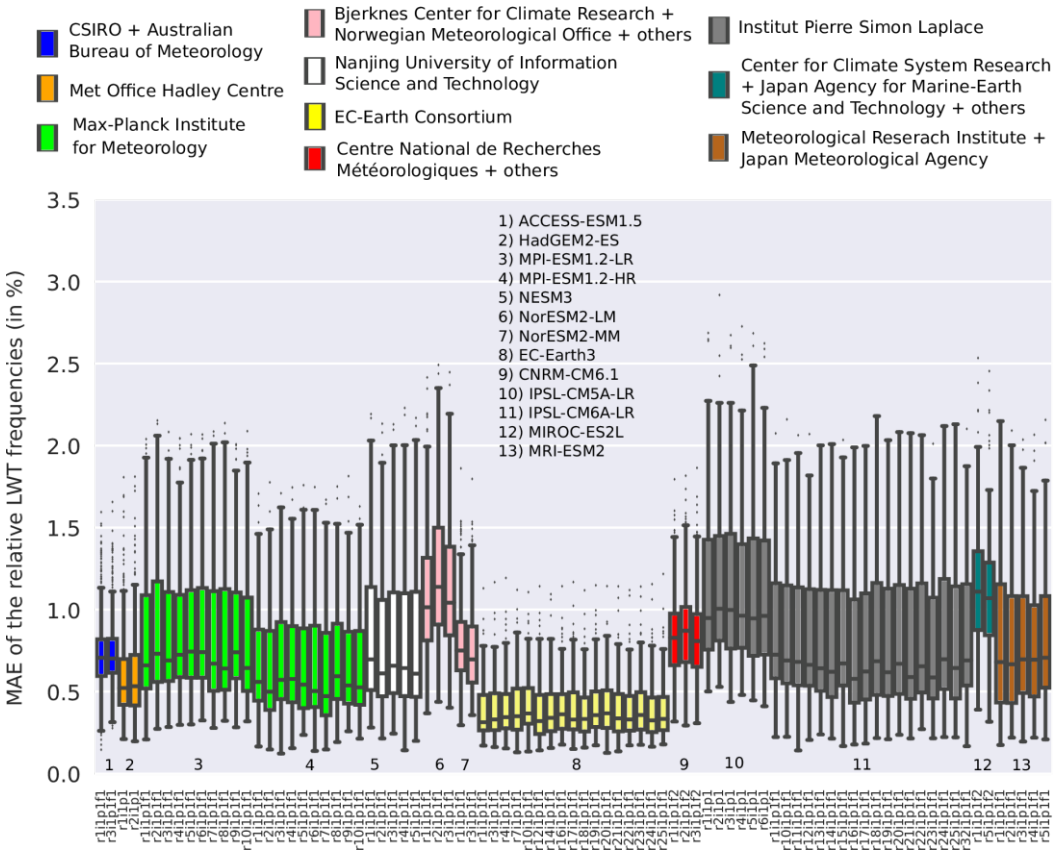

Fig. 3: As Figure 2, but for up to 18 runs of the indicated GCM configurations. Here, colors indicate institutions and the GCM names are numbered.

Figure 5b shows the relationship between the *model complexity score* proposed above, ranging between 8 and 19 for the individual model configurations, and the median model performance. No apparent relationship is found and the more complex versions of a given model family perform approximately equal than the less complex versions. This is an argument in favour of using the more complex model versions, since they provide more realistic representations of the climate system and also produce distinct climate change signals.

Albeit the sensitivity of the results to a switch in the reference reanalysis are generally small for the domain-average results, they do play a considerable role on the grid-box scale for some specific GCMs. Figure 6 visualizes this problem by plotting the JRA-55-based results against those based on ERA5. At some individual grid-boxes of the IB domain, the errors of the EC-Earth family w.r.t. JRA-55 are up to 3 times larger than the respective errors based on ERA5 (panel b). Results for HadGEM3-GC31-MM behave the opposite way, i.e. are favoured by the use of

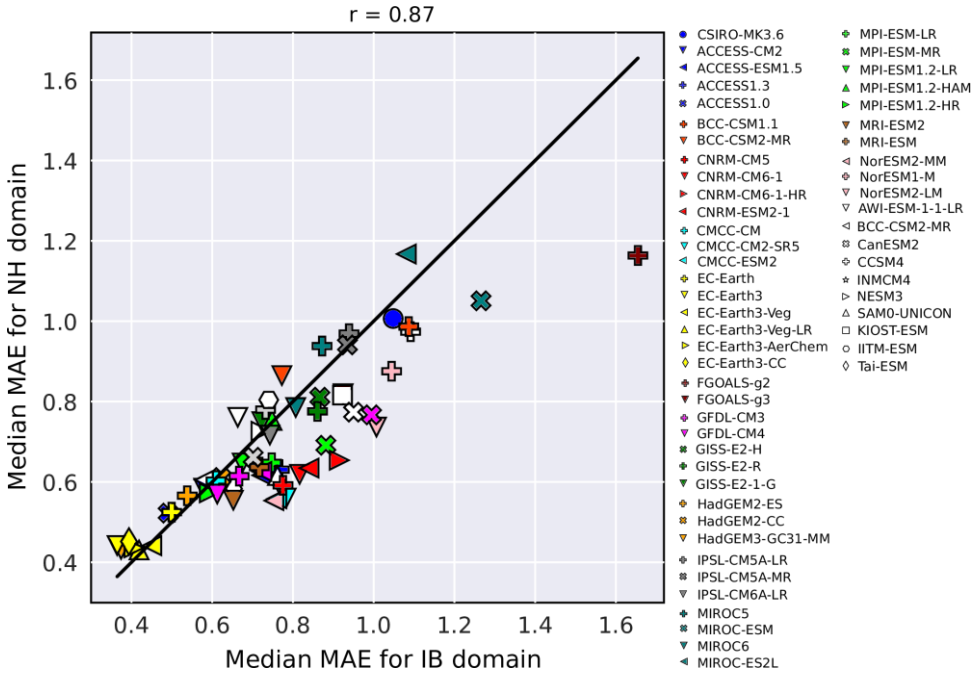

Fig. 4: Median Mean Absolute Error (%) of the relative LWT frequencies over the Iberian Peninsula domain plotted against the corresponding median error for a larger domain covering the northern hemishpere extratropics, obtained from Brands (2022a). Results are with respect to JRA-55.

JRA-55 as reference dataset (panel c), whereas the results of the MPI-ESM1.2-LR are expected, i.e. genearlly not favoured by the choice of a specificd reanalysis (panel a), which is the case for most of the other GCMs. The reasons for such reanlysis "affinities" are speculative and deserve further investigation. The use of the same atmospheric model in the GCM and reanalysis may play a role for EC-Earth thriving to ERA5 since both using ECWMF IFS. Following the same reasoning, however, MRI-ESM1 should thrive towards JRA-55 (both use Japan Meteorological Agency's Global Spectral Model), but this behaviour is surprisingly *not* observed. An alternative explanation is thus that "AGCM sharing" per sé does not lead to similar model errors and that the observed affinities found for EC-Earth might reside on model comparisons (tuning) mainly with ECWMF reanalysis products.

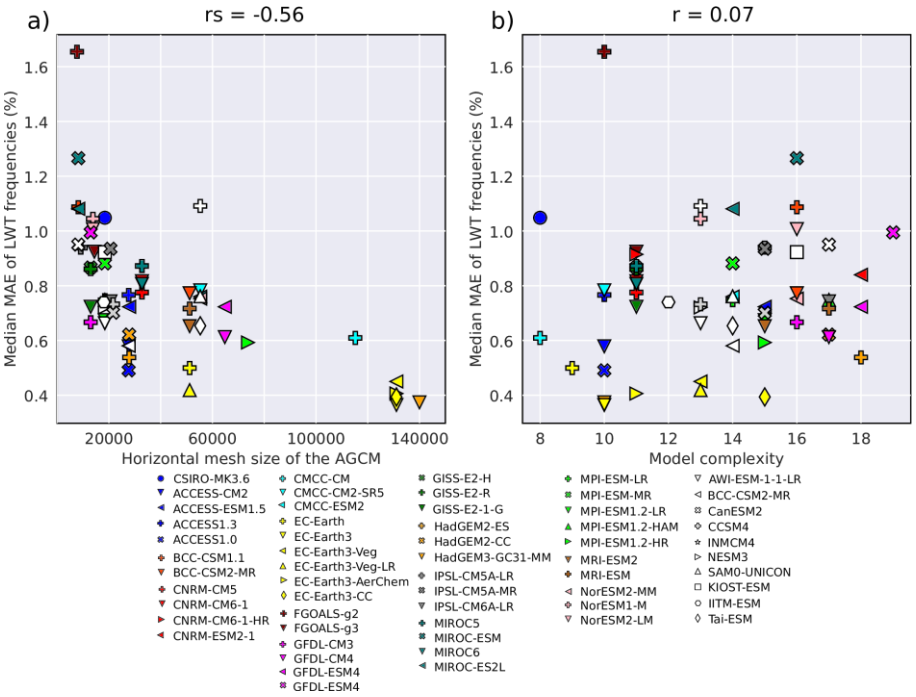

Fig. 5: Relationship between the median performance of the coupled model configuration over the Iberian Peninsula domain and (a) the horizontal mesh size of the atmospheric component or (b) the coupled model complexity score described in Section 2. Model performance is w.r.t. JRA-55. CNRM-CM6-1-HR and CNRM-ESM2-1 are out of scale in panel (a) due to their very fine resolution in the atmosphere. Also shown are the Spearman (rs) or Pearson (r) correlation coefficiencts describing the strength the relationships.

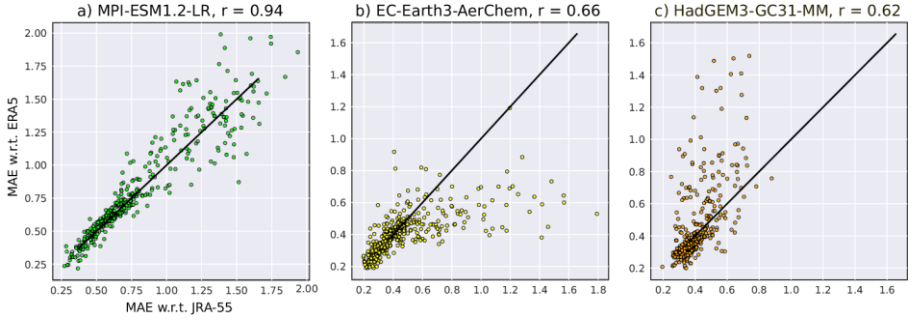

Fig. 6: Relationship between the grid-box-scale model errors obtained with JRA-55 and the errors obtained with ERA5 for 3 distinct GCMs. Points below (above) the diagonal indicate more favourable results if validated against ERA5 (JRA-55), respectively. Results are for the Iberian Peninsula domain.

4. CONCLUSIONS

The present study provides a short summary of global climate model performance in terms of typical atmospheric circulation patterns, tailored to the Iberian Peninsula, at the onset of CMIP6. The model ranking and possibly also the proposed model *complexity* estimates should help to make informed decisions on which GCMs to choose in case the "model democracy" paradigm is not adopted or cannot by adopted for whatever reason, e.g. due to limited resources. The results are largely in agreement with those obtained in a parent study conducted on hemispheric scale. The model metadata archive placed at https://github.com/SwenBrands/gcm-metadata-for-cmip should help to avoid black-box use of the many available GCM configurations and also to channel these configurations to their specific users. This effort is currently under-way and the interested reader is invited to actively participate. Overall, we are intending to inform regional climatologists in a more efficient and complete way than was done at the onset of CMIP5.

ACKNOWLEDGEMENTS

The authors are gradeful to the model and reanlysis development teams for publicly sharing their data and for checking the GCM metadata associated with this study.

REFERENCES

Brands, S. (2022a). A circulation-based performance atlas of the CMIP5 and 6 models for regional climate studies in the Northern Hemisphere mid-to-high latitudes. Geoscientific Model Development 15: 1375–1411, DOI: 10.5194/gmd-15-1375-2022

Brands S. (2022b): A circulation-based performance atlas of the CMIP5 and 6 models for regional climate studies in the northern hemisphere [Data set], version 4. Zenodo. DOI: 10.5281/zenodo.6412397.

Brands S. (2022c): Python code to calculate Lamb circulation types for the northern hemisphere derived from historical CMIP simulations and reanalysis data [Code]. Zenodo. DOI: 10.5281/zenodo.4555367.

Eyring, V; Bony, S; Meehl, G. A.; Senior, C. A.; Stevens, B.; Stouffer, R. J.; Taylor, K. E. (2016). Overview of the Coupled Model Intercomparison Project Phase 6 (CMIP6) experimental design and organization. Geoscientific Model Development 9: 1937-1958. DOI: 10.5194/gmd-9-1937-2016.

Fernández, J.; Frías, M.D.; Cabos, W.D. *et al.* (2019). Consistency of climate change projections from multiple global and regional model intercomparison projects. Climate Dynamics 52: 1139–1156. DOI: 10.1007/s00382-018-4181-8.

Hersbach, H.; Bell, B.; Berrisford, P. et al. (2020). The ERA5 global reanalysis. Quarterly Journal of the Royal Meteorological Society 146: 1999-2049. DOI: 10.1002/qj.3803.

Taylor, K. E.; Stouffer, R. J.; Meehl, G. A. (2012). An Overview of CMIP5 and the Experiment Design. Bulletin of the American Meteorological Society 93(4): 485-498. DOI: 10.1175/BAMS-D-11-00094.1.

Jenkinson, A; Collison, F. (1977). An Initial Climatology of Gales over the North Sea. Synoptic Climatology Branch Memorandum 62, Meteorological Office, Bracknell, UK.

Kobayashi, S.; Ota, Y.; Harada, Y. et al. (2015). The JRA-55 Reanalysis: General Specifications and Basic Characteristics, Journal of the Meteorological Society of Japan Ser. II 93: 5-48. DOI: 10.2151/jmsj.2015-001.

Kawamiya, M.; Hajima, T.; Tachiiri, K.; Watanabe, S.; Yokohata, T. (2020). Two decades of Earth system modeling with an emphasis on Model for Interdisciplinary Research on Climate (MIROC). *Progress in Earth Planet Science* 7(64). DOI: 10.1186/s40645-020-00369-5.

APPENDIX

Principal applied model runs and atmospheric sub-model families used therein (AGCM), median performance for the Iberian Peninsula domain w.r.t. JRA-55 or ERA5 and model complexity scores proposed in Brands (2022a). The AGCMs used in the applied reanalyses are provided at the bottom. A common AGCM in the GCM and reanalysis is indicated by bold.

GCM	Run	AGCM family	JRA-55	ERA5	Complexity
CSIRO-MK3.6	r1i1p1	CSIRO-MK	1.05	1.05	8
ACCESS1.0	r1i1p1	HadGEM / UM	0.49	0.48	10
ACCESS1.3	r1i1p1	HadGEM / UM	0.77	0.73	10
ACCESS-CM2	r1i1p1f1	HadGEM / UM	0.58	0.55	10
ACCESS-ESM1.5	r1i1p1f1	HadGEM / UM	0.72	0.71	15
HadGEM2-ES	r1i1p1	HadGEM / UM	0.54	0.52	18
HadGEM2-CC	r1i1p1	HadGEM / UM	0.62	0.58	17
HadGEM3-GC31-MM	r1i1p1f3	HadGEM / UM	0.37	0.36	10
KACE1.0-G	r1i1p1f1	HadGEM / UM	0.58	0.6	14
FGOALS-g2	r1i1p1	GAMIL	1.65	1.66	10
FGOALS-g3	r3i1p1f1	GAMIL	0.92	0.91	11
MPI-ESM-LR	r1i1p1	ECHAM	0.75	0.76	14
MPI-ESM-MR	r1i1p1	ECHAM	0.88	0.89	14
MPI-ESM1.2-LR	r1i1p1f1	ECHAM	0.67	0.69	15
MPI-ESM1.2-HR	r1i1p1f1	ECHAM	0.59	0.57	15
MPI-ESM-1-2-HAM	r1i1p1f1	ECHAM	0.75	0.77	17
AWI-ESM-1-1-LR	r1i1p1f1	ECHAM	0.66	0.67	13
NESM3	r1i1p1f1	ECHAM	0.72	0.74	13
CMCC-CM	r1i1p1	ECHAM	0.61	0.58	8
CMCC-CM2-SR5	r1i1p1f1	CAM	0.78	0.77	10
CMCC-ESM2	r1i1p1f1	CAM	0.76	0.75	14
CCSM4	r1i1p1	CAM	1.09	1.12	13
NorESM1-M	r1i1p1f1	CAM	1.04	1.04	13
NorESM2-LM	r1i1p1f1	CAM	1.01	1.03	16
NorESM2-MM	r1i1p1f1	CAM	0.75	0.75	16
SAM0-UNICON	r1i1p1f1	CAM	0.76	0.77	14
TaiESM1	r1i1p1f1	CAM	0.65	0.64	14
BCC-CSM1.1	r1i1p1	BCC-AGCM / CAM	1.09	1.08	16
BCC-CSM2-MR	r1i1p1f1	BCC-AGCM / CAM	0.77	0.78	16
CNRM-CM5	r1i1p1	ARPECHE	0.78	0.79	11
CNRM-CM6-1	r1i1p1f2	ARPECHE	0.82	0.83	11
CNRM-CM6-1-HR	r1i1p1f2	ARPECHE	0.91	0.91	11
CNRM-ESM2-1	r1i1p1f2	ARPECHE	0.84	0.83	18

EC-Earth2.3	**r12i1p1**	**IFS**	**0.50**	**0.49**	**9**
EC-Earth3	**r1i1p1f1**	**IFS**	**0.36**	**0.33**	**10**
EC-Earth-Veg	**r1i1p1f1**	**IFS**	**0.45**	**0.40**	**13**
EC-Earth-Veg-LR	**r1i1p1f1**	**IFS**	**0.42**	**0.41**	**13**
EC-Earth-AerChem	**r1i1p1f1**	**IFS**	**0.41**	**0.41**	**11**
EC-Earth-CC	**r1i1p1f1**	**IFS**	**0.39**	**0.35**	**15**
GFDL-CM3	r1i1p1	GFDL-AM	0.67	0.67	16
GFDL-CM4	r1i1p1f1	GFDL-AM	0.61	0.62	17
GFDL-ESM2G	r1i1p1	GFDL-AM	0.99	1.00	19
GFDL-ESM4	r1i1p1f1	GFDL-AM	0.72	0.74	18
KIOST-ESM	r1i1p1f1	GFDL-AM	0.92	0.95	16
GISS-E2-H	r6i1p1	ModelE2 AGCM	0.87	0.87	11
GISS-E2-R	r6i1p1	ModelE2 AGCM	0.86	0.85	11
GISS-E2.1-G	r1i1p1f1	ModelE2 AGCM	0.72	0.74	11
IPSL-CM5A-LR	r1i1p1	LMDZ	0.94	0.95	15
IPSL-CM5A-MR	r1i1p1	LMDZ	0.94	0.98	15
IPSL-CM6A-LR	r1i1p1f1	LMDZ	0.74	0.74	17
MIROC5	r1i1p1	MIROC-AGCM	0.87	0.87	11
MIROC6	r3i1p1f1	MIROC-AGCM	0.81	0.82	11
MIROC-ESM	r1i1p1	MIROC-AGCM	1.27	1.29	16
MIROC-ES2L	r5i1p1f2	MIROC-AGCM	1.08	1.06	14
MRI-ESM1	**r1i1p1**	**GSMUV / MRI-AGCM**	**0.72**	**0.72**	**17**
MRI-ESM2.0	**r1i1p1f1**	**GSMUV / MRI-AGCM**	**0.65**	**0.68**	**15**
INM-CM4	r1i1p1	INM-AM	0.73	0.68	13
INM-CM5	r2i1p1f1	INM-AM	0.7	0.68	15
CanESM2	r1i1p1	CanAM	0.95	0.97	17
IITM-ESM	r1i1p1f1	GFS	0.74	0.76	12
		Reanalyses			
JRA-55		**JMA-GSM**			
ERA5		**IFS**			
ERA-Interim		**IFS**			